Acta Mech 235, 2695–2714 (2024)
https://doi.org/10.1007/s00707-024-03858-6

ORIGINAL PAPER

Mofareh Hassan Ghazwani · Ali Alnujaie · Mehmet Avcar · Pham Van Vinh

Examination of the high-frequency behavior of functionally graded porous nanobeams using nonlocal simple higher-order shear deformation theory

Received: 23 September 2023 / Revised: 28 December 2023 / Accepted: 5 January 2024 / Published online: 7 February 2024

Abstract The primary objective of this paper is to examine the free vibration behaviors of functionally graded nanobeams with porosity while considering nonlocal parameters. The nanobeams are built of functionally graded materials, having material features that change smoothly over the beam's thickness. To illustrate how porosity is distributed throughout the body of the beams, four different forms of porosity distribution are taken into consideration. Eringen's nonlocal parameter elasticity theory and Hamilton's principle are used to establish the governing equations of the motion of the functionally graded porous nanobeams. Then, the closed-form solution of Navier is used to solve the eigenvalue problems to find the frequencies of the functionally graded porous nanobeams. A comprehensive parametric study is also carried out to demonstrate the influence of geometric parameters, material gradient index, and nonlocal parameters on low- and high-frequency vibration behaviors of the functionally graded porous nanobeams. The results of the vibration of the functionally graded porous nanobeams undergoing the low- and high-frequency conditions can serve as benchmarks for applications of such structures in engineering and for future work.

1 Introduction

Functionally graded materials (FGMs) have drawn a lot of interest recently because of their numerous uses and distinctive mechanical characteristics [1–3]. FGMs exhibit a spatial variation in composition, resulting in tailored properties that can be manipulated to optimize performance across a range of engineering and scientific specialties. The study of FGMs has paved the way for innovative solutions in fields such as aerospace engineering, structural mechanics, biomechanics, and nanotechnology [4–12]. Particularly intriguing are functionally graded (FG) nanostructures, which extend these advantages to the nanoscale, enabling enhanced material functionality and novel applications.

The analysis of nanostructures, including nanoplates, nano-shells, and nanobeams, has been the subject of intensive research. Various theories have been employed to study their mechanical behavior, ranging from classical elasticity to more advanced approaches that account for size-dependent and nonlocal effects [13–15]. These theories have revealed a capital of insights into the mechanics of nanostructures, shedding light on phenomena such as size-dependent stiffness, surface effects, and nonlocal behavior [16–18]. Therefore, under-

M. H. Ghazwani · A. Alnujaie
Mechanical Engineering Department, Faculty of Engineering, Jazan University, P. O. Box 45142, Jazan, Kingdom of Saudi Arabia

M. Avcar
Department of Civil Engineering, Faculty of Engineering, Suleyman Demirel University, Cunur, 32260 Isparta, Türkiye

P. Van Vinh (✉)
Department of Solid Mechanics, Le Quy Don Technical University, Hoang Quoc Viet, Hanoi, Vietnam
e-mail: phamvanvinh@lqdtu.edu.vn

standing the vibration characteristics of nanostructures has become essential for designing and optimizing nanoscale devices and systems.

In recent years, investigating the vibration problems in nanostructures has become particularly prominent. Nanobeams, which have become fundamental building blocks in many nanoscale applications, have been of particular interest. Notably, FG nanobeams exhibit distinct behavior because of the gradual variation of material features through the thickness. Eringen [19–22] provided the differential constitutive model and integral constitutive model of the nonlocal elasticity theory (NET), which has been applied by many scientists to analyze nanostructures. By using NET, the nonlocal bending, free vibration, and buckling behaviors of the isotropic and FG nanobeams have been investigated extensively by Eltaher et al. [23], Thai et al. [24], Rahmani et al. [25], Arefi et al. [26], Gholami et al. [27]. Ebrahimi et al. [28–31], and Karami et al. [32]. The effects of the hygrothermal, piezoelectricity, magneto-piezoelectricity, and flexoelectricity on the mechanical behaviors of the nanobeams were also investigated carefully. The results of these studies also show that the nonlocal parameters have significant effects on the behaviors of the nanostructures.

It is noticed that the integration of porosity into these structures leads to an additional level of complexity, affecting their mechanical response. Therefore, examining the mechanical behaviors of porous nanobeams has become the focus of researchers' attention. Several studies on the effects of porosity were caried out, for example, Aria et al. [33], Ghobadi et al. [34], Ebrahimi et al. [35], Wang et al. [36, 37], Faghidian et al. [38], Civalek et al. [39], Rastehkenari et al. [40], Chandel et al. [41], Hadji et al. [42], and Akbas [43], and so on. More details on the analysis of the FG nanobeams with and without porosity are reported in the studies of Numanoğlu et al. [44], Şimşek [45], Barati et al. [46], and their references. In those studies, NET and nonlocal strain gradient theory were applied to consider for small-scale effects. The outcomes of these works also demonstrated that the distribution of porosity and coefficient of porosity plays a significant role in the behaviors of the nanostructures.

Consequently, the results of above-mentioned works showed that porosity has considerable influences on the dynamic responses of the FG porous nanobeams and should be investigated more. Additionally, in the above-mentioned studies, only some first modes of the nanobeams, especially the fundamental mode, were investigated. Therefore, despite the growing body of knowledge in this area, a comprehensive study of the vibration behavior of FG porous nanobeams, especially undergoing high-frequency conditions considering the influence of nonlocal parameters, remains an important research gap. Therefore, the present study aims to report this problem by analyzing the free vibration behaviors of FG nanobeams, including porosity, while considering the effects of nonlocal parameters. This investigation not only contributes to the understanding the vibration behavior of FG porous nanobeams but also provides insights into the influence of geometric parameters, material gradient index, and nonlocal parameters on their low- and high-frequency vibration characteristics. The obtained results offer valuable benchmarks for the engineering applications of such structures and guide future research endeavors. By exploring the effects of porosity and considering various material property gradients, this research advances the knowledge base in the field of nano-mechanics and offers practical insights for the design and optimization of nanoscale devices and systems.

2 Theoretical formulation of the problem

2.1 Functionally graded porous nanobeams

In this study, as presented in Fig. 1, an FG porous nanobeam is considered. The porosity distributes through the volume of the nanobeam, with uniform distribution through the longitudinal direction, and non-uniform through the thickness of the nanobeams. The beam's height is h, and the beam's length is L.

The variation of the material characteristics along the thickness of the FG porous nanobeams can be estimated using the simple mixing rule. For the perfect FG nanobeams

$$\begin{aligned} E(z) &= E_{\mathrm{m}} + (E_{\mathrm{c}} - E_{\mathrm{m}})\left(\frac{1}{2} + \frac{z}{h}\right)^{k} \\ \rho(z) &= \rho_{\mathrm{m}} + (\rho_{\mathrm{c}} - \rho_{\mathrm{m}})\left(\frac{1}{2} + \frac{z}{h}\right)^{k} \\ \nu(z) &= \nu_{\mathrm{m}} + (\nu_{\mathrm{c}} - \nu_{\mathrm{m}})\left(\frac{1}{2} + \frac{z}{h}\right)^{k} \end{aligned} \tag{1}$$

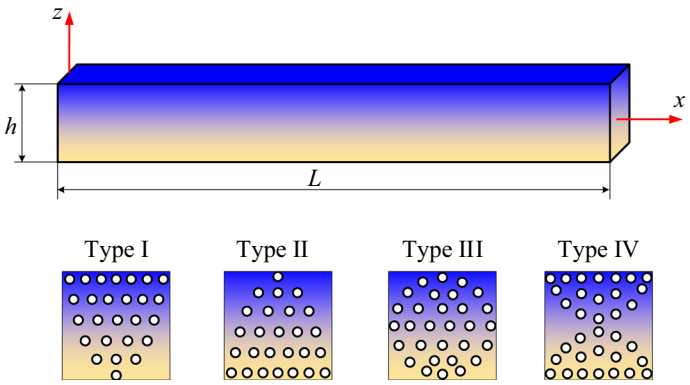

Fig. 1 The model of the FG nanobeams

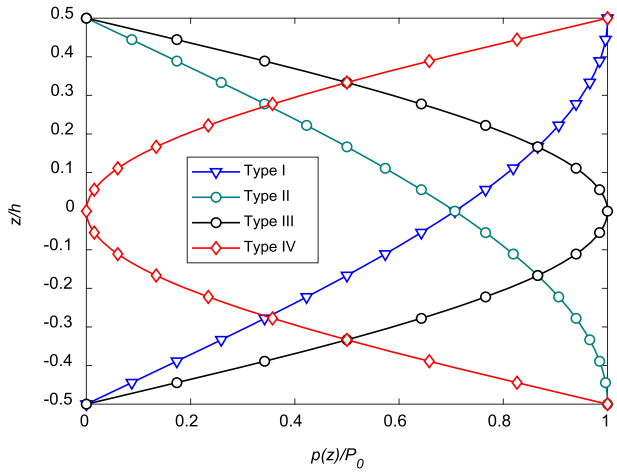

Fig. 2 The porosity distribution throughout the thickness of the FG porous nanobeams

where subscripts c, m denote the ceramic and metal phases, respectively, k is the material gradient index, and E, ρ, ν represent the Young's modulus, mass density, and Poisson's ratio of material, respectively.

The manufacturing process of sintering, which is common in the production of FGMs, is responsible for the formation of voids or porosities within the materials. On the other hand, FGMs can be further improved in terms of weight reduction and energy absorption by introducing porosity while maintaining a significant amount of its strength. Besides, FG porous media can be utilized in several engineering applications, such as enhanced filtration, the automotive industry, and medical implants. Therefore, it is important to introduce the porosity effects at the analysis, testing, and design stage of the FG structures. The distribution of porosity in FG structures can be random or regular. In this study, four common types of distributions, called Type I, II, III, and IV, are utilized to consider the effects of the porosity on the change of the material properties of the FG nanobeams. These distributions are given by the following formulae [47].

$$\begin{cases} \text{Type I} & : p(z) = P_0 \cos\left[\frac{\pi}{2}\left(\frac{z}{h} - 0.5\right)\right] \\ \text{Type II} & : p(z) = P_0 \cos\left[\frac{\pi}{2}\left(\frac{z}{h} + 0.5\right)\right] \\ \text{Type III:} & p(z) = P_0 \cos\left[\pi\left(\frac{z}{h}\right)\right] \\ \text{Type IV:} & p(z) = P_0 - P_0 \cos\left[\pi\left(\frac{z}{h}\right)\right] \end{cases} \tag{2}$$

where $p(z)$ is the function that demonstrates the porosity distribution throughout the thickness of the FG porous nanobeams, and P_0 is the maximum porosity coefficient. The illustration of the functions of the porosity distributions are presented in Fig. 2.

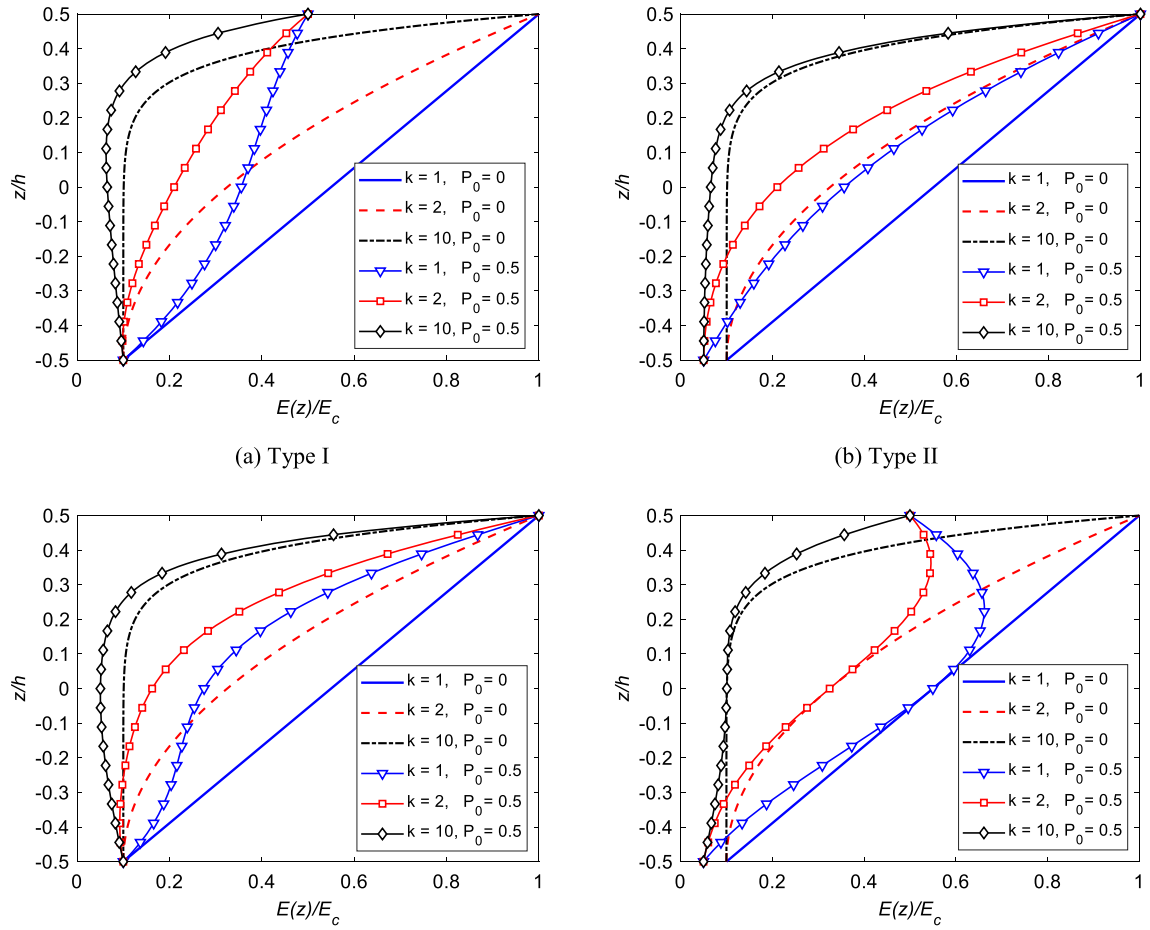

(a) Type I (b) Type II

(c) Type III (d) Type IV

Fig. 3 The variation of effective Young's modulus throughout the thickness of the FG porous nanobeams

The effective material characteristics of the FG porous nanobeams are computed as follows:

$$\begin{aligned} E(z) &= \left[E_{\mathrm{m}} + (E_{\mathrm{c}} - E_{\mathrm{m}})\left(\frac{1}{2} + \frac{z}{h}\right)^{k}\right](1 - p(z)) \\ \rho(z) &= \left[\rho_{\mathrm{m}} + (\rho_{\mathrm{c}} - \rho_{\mathrm{m}})\left(\frac{1}{2} + \frac{z}{h}\right)^{k}\right](1 - p(z)) \end{aligned} \tag{3}$$

According to some published works, the effects of the Poisson's ratio on the mechanical behaviors of the structures are small [48–50]; therefore, in this study, the Poisson's ratio is assumed to be independent of porosity. Figure 3 shows the variation of the effective Young's modulus, $E(z)$, through the thickness of the FG porous nanobeams with $E_{\mathrm{c}}/E_{\mathrm{m}} = 10$.

2.2 The simple higher-order shear beam theory

To establish the equations of motion of the FG porous nanobeams, a simple higher-order shear deformation theory [51] is used; therefore, the displacement fields of the FG porous nanobeams are as follows:

$$\begin{aligned} u(x,z,t) &= u(x,t) - z\frac{\partial w_b(x,t)}{\partial x} - f(z)\frac{\partial w_s(x,t)}{\partial x} \\ w(x,z,t) &= w_b(x,t) + w_s(x,t) \end{aligned} \tag{4}$$

where $u(x, t)$ denotes the axial displacement, $w_b(x, t)$ and $w_s(x, t)$ describe the bending and shear parts of the transverse displacement of a point at the midplane of the beams. The bending part $w_b(x, t)$ is assumed to be similar to the displacement of the classical beam theory; the shear part $w_s(x, t)$ gives rise to the nonlinear variation of the shear strain γ_{xz} and hence to the shear stress τ_{xz} through the thickness of the beams in such a way that the shear stress τ_{xz} satisfies free condition at the top and bottom surfaces of the beams. The formulation of $f(z)$ is chosen to fulfill the free condition of the shear stress on the top and bottom surfaces of the FG porous nanobeams. In this study, the function $f(z)$ is chosen as follows [52]:

$$f(z) = \frac{5z^3}{3h^2} - \frac{z}{h} \tag{5}$$

The strain fields of the FG porous nanobeams can be expressed as follows:

$$\begin{aligned} \varepsilon_x &= \frac{\partial u}{\partial x} - z\frac{\partial^2 w_b}{\partial x^2} - f\frac{\partial^2 w_s}{\partial x^2} \\ \gamma_{xz} &= g\frac{\partial w_s}{\partial x} \end{aligned} \tag{6}$$

where

$$g(z) = 1 - \frac{\mathrm{d}f(z)}{\mathrm{d}z} \tag{7}$$

It is evident that the simple higher-order shear deformation theory involves only three unknowns, similar to the conventional first-order shear deformation beam theory. In contrast, other higher-order shear deformation beam theories often employ four, five, or even more unknowns. The utilization of a polygonal function, denoted as $f(z)$, introduces nonlinearity in the distribution of transverse shear strain and stress throughout the thickness direction. This polygonal function effectively satisfies traction-free boundary conditions on the top and bottom surfaces of the beam, eliminating the need for a shear correction factor—a factor dependent on material gradient, as noted by Nguyen et al. [53] and Menaa et al. [54]. In comparison to other functions like hyperbolic, trigonometric, or exponential functions, the polygonal function stands out for its simplicity and ability to yield a high convergence rate during integration through the thickness of the beam.

2.3 Nonlocal constitutive relations

To consider the small-scale influences on the mechanical behaviors of the FG porous nanobeams, Eringen's nonlocal theory [19–22] is adopted herein. According to Eringen's nonlocal theory, the stress at a location is determined by the stresses at all of the body's neighboring points; hence, the nonlocal stress tensor σ_{ij}^{nl} at a point x is obtained via the local stress tensor σ_{ij}^{l} as the following formula

$$\sigma_{ij}^{nl} = \int_V \alpha\left(\left|\mathbf{x}' - \mathbf{x}\right|, \tau\right)\sigma_{ij}^{l}\mathrm{d}V(\mathbf{x}') \tag{8}$$

where α is the kernel function, which contains the small-scale effects incorporating into constitutive equations the nonlocal effects at the reference point $\mathbf{x}$ produced by local strain at the source $\mathbf{x}'$. This function depends on two variables $\left|\mathbf{x}' - \mathbf{x}\right|$ and τ, where $\left|\mathbf{x}' - \mathbf{x}\right|$ is the distance in Euclidean form, $\tau = e_0 a/L$ is a material constant that depends on internal and external characteristic length (such as the lattice spacing and wavelength). The parameter e_0 is vital for the validity of nonlocal models. This parameter is determined by matching the dispersion curves based on atomistic models. The classical stress tensor is defined as follows:

$$\sigma_{ij}^{l} = C_{ijkl} : \varepsilon_{kl} \tag{9}$$

where C_{ijkl} denote the fourth order elasticity tensor. By choosing the appropriate kernel function, Eringen showed that the nonlocal constitutive equation in integral form can be represented in an equivalent differential form as

$$(1 - \mu\nabla^2)\sigma_{ij}^{nl} = \sigma_{ij}^{l} \tag{10}$$

where $\mu = (e_0 a)^2$ is the nonlocal parameter, which includes the small-scale effect. The nonlocal constitutive relation for a nonlocal beam may be expressed as follows:

$$\left(1 - \mu\nabla^2\right)\begin{Bmatrix}\sigma_x\\ \tau_{xz}\end{Bmatrix} = \begin{bmatrix}\Theta_{11} & 0\\ 0 & \Theta_{55}\end{bmatrix}\begin{Bmatrix}\varepsilon_x\\ \gamma_{xz}\end{Bmatrix} \tag{11}$$

where

$$\Theta_{11} = E(z),\ \Theta_{55} = G(z) = \frac{E(z)}{2(1+\nu(z))} \tag{12}$$

2.4 Equations of motion in terms of displacements

The following application of Hamilton's principle is used to generate the equations of motion of the FG porous nanobeams:

$$0 = \int_0^T (\delta\Pi - \delta T)\mathrm{d}t \tag{13}$$

where $\delta\Pi$ and δT are the variations of the strain energy and the kinetic energy, respectively.

The variation of the strain energy can be obtained as the follow:

$$\delta\Pi = \int_0^L \int_A (\sigma_x \delta\varepsilon_x + \tau_{xz}\delta\gamma_{xz})\mathrm{d}A\mathrm{d}x \tag{14}$$

After some mathematical operations and simplifications, one gets the following equation:

$$\delta\Pi = \int_0^L \left(N\frac{\partial\delta u}{\partial x} - M\frac{\partial^2\delta w_\mathrm{b}}{\partial x^2} - P\frac{\partial^2\delta w_\mathrm{s}}{\partial x^2} + Q\frac{\partial\delta w_\mathrm{s}}{\partial x}\right)\mathrm{d}x \tag{15}$$

where N, M, P and Q are the stress resultants which can be calculated by

$$\begin{aligned} N &= \int_A \sigma_x \mathrm{d}A;\ M = \int_A z\sigma_x \mathrm{d}A;\\ P &= \int_A (f)\sigma_x \mathrm{d}A;\ Q = \int_A (g)\tau_{xz}\mathrm{d}A \end{aligned} \tag{16}$$

The variation of the kinetic energy of the FG nanobeams can be expressed as follows:

$$\delta T = \int_0^L \int_A (\dot{u}\delta\dot{u} + \dot{w}\delta\dot{w})\rho\mathrm{d}A\mathrm{d}x \tag{17}$$

$$\begin{aligned} \delta T = \int_0^L \int_A &\left(\dot{u} - z\frac{\partial\dot{w}_\mathrm{b}}{\partial x} - f\frac{\partial\dot{w}_\mathrm{s}}{\partial x}\right)\rho(z)\left(\delta\dot{u} - z\frac{\partial\delta\dot{w}_\mathrm{b}}{\partial x} - f\frac{\partial\delta\dot{w}_\mathrm{s}}{\partial x}\right)\\ &+(\dot{w}_\mathrm{b} + \dot{w}_\mathrm{s})\rho(\delta\dot{w}_\mathrm{b} + \delta\dot{w}_\mathrm{s})\mathrm{d}A\mathrm{d}x \end{aligned} \tag{18}$$

After some mathematical operations and simplifications, one gets the following equation:

$$\begin{aligned} \delta T = \int_0^L &[I_0(\dot{u}\delta\dot{u} + (\dot{w}_\mathrm{b} + \dot{w}_\mathrm{s})(\delta\dot{w}_\mathrm{b} + \delta\dot{w}_\mathrm{s})) + I_1\left(\dot{u}\frac{\partial\delta\dot{w}_\mathrm{b}}{\partial x} + \frac{\partial\dot{w}_\mathrm{b}}{\partial x}\delta\dot{u}\right) + I_2\left(\dot{u}\frac{\partial\delta\dot{w}_\mathrm{s}}{\partial x} + \frac{\partial\dot{w}_\mathrm{s}}{\partial x}\delta\dot{u}\right)\\ &+I_3\left(\frac{\partial\dot{w}_\mathrm{b}}{\partial x}\frac{\partial\delta\dot{w}_\mathrm{b}}{\partial x}\right) + I_4\left(\frac{\partial\dot{w}_\mathrm{b}}{\partial x}\frac{\partial\delta\dot{w}_\mathrm{s}}{\partial x} + \frac{\partial\dot{w}_\mathrm{s}}{\partial x}\frac{\partial\delta\dot{w}_\mathrm{b}}{\partial x}\right) + I_5\left(\frac{\partial\dot{w}_\mathrm{s}}{\partial x}\frac{\partial\delta\dot{w}_\mathrm{s}}{\partial x}\right)\Bigg]\mathrm{d}x \end{aligned} \tag{19}$$

where

$$I_0 = \int_A \rho(z)\mathrm{d}A;\ I_1 = \int_A \rho(z)(-z)\mathrm{d}A;\ I_2 = \int_A \rho(z)(-f)\mathrm{d}A;$$
$$I_3 = \int_A \rho(z)\left(z^2\right)\mathrm{d}A;\ I_4 = \int_A \rho(z)(zf)\mathrm{d}A;\ I_5 = \int_A \rho(z)\left(f^2\right)\mathrm{d}A \tag{20}$$

Substituting Eqs. (15) and (19) into Eq. (13) and integrating by parts, the equilibrium equations of the FG porous nanobeams are found as follows:

$$\begin{aligned}
&\delta u: -\frac{\partial N}{\partial x} = -I_0\ddot{u} - I_1\frac{\partial \ddot{w}_\mathrm{b}}{\partial x} - I_2\frac{\partial \ddot{w}_\mathrm{s}}{\partial x};\\
&\delta w_\mathrm{b}: -\frac{\partial^2 M}{\partial x^2} = -I_0(\ddot{w}_\mathrm{b} + \ddot{w}_\mathrm{s}) + I_1\frac{\partial \ddot{u}}{\partial x} + I_3\frac{\partial^2 \ddot{w}_\mathrm{b}}{\partial x^2} + I_4\frac{\partial^2 \ddot{w}_\mathrm{s}}{\partial x^2};\\
&\delta w_\mathrm{s}: -\frac{\partial^2 P}{\partial x^2} - \frac{\partial Q}{\partial x} = -I_0(\ddot{w}_\mathrm{b} + \ddot{w}_\mathrm{s}) + I_2\frac{\partial \ddot{u}}{\partial x} + I_4\frac{\partial^2 \ddot{w}_\mathrm{b}}{\partial x^2} + I_5\frac{\partial^2 \ddot{w}_\mathrm{s}}{\partial x^2}.
\end{aligned} \tag{21}$$

The boundary conditions of the present theory are as follows:

$$\begin{aligned}
&\text{Specify } u \quad \text{or } N\\
&\text{Specify } w_\mathrm{b} \quad \text{or } V_\mathrm{b} \equiv \tfrac{\partial M}{\partial x} + I_3\tfrac{\partial \ddot{w}_\mathrm{b}}{\partial x}\\
&\text{Specify } w_\mathrm{s} \quad \text{or } V_\mathrm{s} \equiv \tfrac{\partial P}{\partial x} + Q + I_5\tfrac{\partial \ddot{w}_\mathrm{s}}{\partial x}\\
&\text{Specify } \tfrac{\partial w_\mathrm{b}}{\partial x} \text{ or } M\\
&\text{Specify } \tfrac{\partial w_\mathrm{s}}{\partial x} \text{ or } P
\end{aligned} \tag{22}$$

By substituting Eq. (6) into Eq. (11) and the subsequent results into Eq. (16), the stress resultants of the FG porous nanobeams are obtained as follows

$$\begin{Bmatrix} N \\ M \\ P \end{Bmatrix} - \mu\nabla^2 \begin{Bmatrix} N \\ M \\ P \end{Bmatrix} = \begin{bmatrix} A & B & C \\ B & D & E \\ C & E & F \end{bmatrix} \begin{Bmatrix} \frac{\partial u}{\partial x} \\ -\frac{\partial^2 w_\mathrm{b}}{\partial x^2} \\ -\frac{\partial^2 w_\mathrm{s}}{\partial x^2} \end{Bmatrix} \tag{23}$$

$$Q - \mu\nabla^2 Q = S\frac{\partial w_\mathrm{s}}{\partial x} \tag{24}$$

where

$$A = \int_A \Theta_{11}\mathrm{d}A;\ B = \int_A \Theta_{11}(z)\mathrm{d}A;\ D = \int_A \Theta_{11}\left(z^2\right)\mathrm{d}A;$$
$$C = \int_A \Theta_{11}(f)\mathrm{d}A;\ E = \int_A \Theta_{11}(zf)\mathrm{d}A;\ F = \int_A \Theta_{11}\left(f^2\right)\mathrm{d}A \tag{25}$$

$$S = \int_A \Theta_{55}(g)^2\mathrm{d}A \tag{26}$$

Inserting Eqs. (23) and (24) into Eq. (21), the equations of motion of the FG porous nanobeams in terms of displacements are obtained as:

$$\begin{aligned}
&\delta u: \ A\frac{\partial^2 u}{\partial x^2} - B\frac{\partial^3 w_\mathrm{b}}{\partial x^3} - C\frac{\partial^3 w_\mathrm{s}}{\partial x^3} \\
&= \left(1-\mu\nabla^2\right)\left(I_0\ddot{u} + I_1\frac{\partial \ddot{w}_\mathrm{b}}{\partial x} + I_2\frac{\partial \ddot{w}_\mathrm{s}}{\partial x}\right), \\
&\delta w_\mathrm{b}: B\frac{\partial^3 u}{\partial x^3} - D\frac{\partial^4 w_\mathrm{b}}{\partial x^4} - E\frac{\partial^4 w_\mathrm{s}}{\partial x^4} \\
&= \left(1-\mu\nabla^2\right)\left(I_0(\ddot{w}_\mathrm{b}+\ddot{w}_\mathrm{s}) - I_1\frac{\partial \ddot{u}}{\partial x} - I_3\frac{\partial^2 \ddot{w}_\mathrm{b}}{\partial x^2} - I_4\frac{\partial^2 \ddot{w}_\mathrm{s}}{\partial x^2}\right), \\
&\delta w_\mathrm{s}: C\frac{\partial^3 u}{\partial x^3} - E\frac{\partial^4 w_\mathrm{b}}{\partial x^4} - F\frac{\partial^4 w_\mathrm{s}}{\partial x^4} + S\frac{\partial^2 w_\mathrm{s}}{\partial x^2} \\
&= \left(1-\mu\nabla^2\right)\left(I_0(\ddot{w}_\mathrm{b}+\ddot{w}_\mathrm{s}) - I_2\frac{\partial \ddot{u}}{\partial x} - I_4\frac{\partial^2 \ddot{w}_\mathrm{b}}{\partial x^2} - I_5\frac{\partial^2 \ddot{w}_\mathrm{s}}{\partial x^2}\right).
\end{aligned} \tag{27}$$

3 Analytical solution of the problem

Since this study considers a simply supported FG porous nanobeams, the Navier's solution method is used to solve the equations of motion, and the following formulas are employed to represent the unknown displacement functions of the beams:

$$\begin{aligned}
u(x,t) &= \sum_{m=1}^{\infty} U_m \cos\alpha_m x \sin\omega t \\
w_\mathrm{b}(x,t) &= \sum_{m=1}^{\infty} Wb_m \sin\alpha_m x \sin\omega t \\
w_\mathrm{s}(x,t) &= \sum_{m=1}^{\infty} Ws_m \sin\alpha_m x \sin\omega t
\end{aligned} \tag{28}$$

where $\alpha_m = m\pi/L$, ω is the frequency of the nanobeams, U_m, Wb_m, Ws_m are the unknown coefficients.

Substituting Eq. (28) into Eq. (27), the subsequent equation is gotten and the results for vibration behaviors of the FG porous nanobeams are found from the solution of it:

$$\left(\begin{bmatrix} k_{11} & k_{12} & k_{13} \\ k_{12} & k_{22} & k_{23} \\ k_{13} & k_{23} & k_{33} \end{bmatrix} - \omega^2\vartheta \begin{bmatrix} m_{11} & m_{12} & m_{13} \\ m_{12} & m_{22} & m_{23} \\ m_{13} & m_{23} & m_{33} \end{bmatrix}\right)\begin{Bmatrix} U_m \\ Wb_m \\ Ws_m \end{Bmatrix} = \begin{Bmatrix} 0 \\ 0 \\ 0 \end{Bmatrix} \tag{29}$$

where

$$\begin{aligned}
&k_{11} = \alpha^2 A;\ k_{12} = -\alpha^3 B;\ k_{13} = -C\alpha^3; \\
&k_{22} = \alpha^4 D;\ k_{23} = \alpha^4 E;\ k_{33} = \alpha^2\left(F\alpha^2 + S\right); \\
&m_{11} = I_0;\ m_{12} = I_1\alpha;\ m_{13} = I_2\alpha; \\
&m_{22} = I_3\alpha^2 + I_0;\ m_{23} = I_4\alpha^2 + I_0;\ m_{33} = I_5\alpha^2 + I_0; \\
&\vartheta = \left(\alpha^2\mu + 1\right).
\end{aligned} \tag{30}$$

4 Numerical results

In this section, at first illustrative examples regarding the free vibration behaviors of the FG porous beams and FG nanobeams are considered to verify the validity of the existing theory and formulations. Then, the

proposed algorithm is applied to study the free vibration behaviors of the FG porous nanobeams, and the high-frequency and of low-frequency behaviors of the FG porous nanobeams are compared. By this way, some new important results are provided to help researchers and engineers understand more clearly the response of the FG porous nanobeams at high-frequency conditions.

4.1 Validations

Firstly, a simply supported FG porous beams made from Al_2O_3/Al with the uniform distributed porosity is considered. The material features of the ceramic phase, Al_2O_3, are $E_c = 380$ GPa, $\rho_c = 3960$ kg/m^3, $\nu_c = 0.3$; for the metal phase, Al, are $E_m = 70$ GPa, $\rho_m = 2702$ kg/m^3, $\nu_m = 0.3$, and the length of the beam is $L = 10h$, the nonlocal parameter is given $\mu = 0$ (local beams). Two types of porosity distributions, even and uneven porosity distributions, are considered. The material properties of the FGP beam are expressed as follows:

For even porosity distribution [42]:

$$\begin{aligned} E(z) &= \left[E_m + (E_c - E_m)\left(\frac{1}{2} + \frac{z}{h}\right)^k\right] - \frac{1}{2}P_0(E_c + E_m) \\ \rho(z) &= \left[\rho_m + (\rho_c - \rho_m)\left(\frac{1}{2} + \frac{z}{h}\right)^k\right] - \frac{1}{2}P_0(\rho_c + \rho_m) \end{aligned} \tag{31}$$

Table 1 Comparison of the non-dimensional frequency of the FG porous beams versus different porosity distribution and *L/h*

L/h	Sources	Even porosity			Uneven porosity		
		$P_0 = 0$	$P_0 = 0.1$	$P_0 = 0.2$	$P_0 = 0$	$P_0 = 0.1$	$P_0 = 0.2$
5	Hadji et al. [42]	3.6264	3.4418	3.1489	3.6264	3.6069	3.5785
	Present	3.6264	3.4418	3.1489	3.6264	3.6070	3.5785
20	Hadji et al. [42]	3.8361	3.6335	3.3123	3.8361	3.8226	3.8004
	Present	3.8361	3.6335	3.3123	3.8361	3.8226	3.8004

Table 2 Comparison non-dimensional fundamental frequency of the FG nanobeams versus different *L/h* and μ

L/h	$\mu \times 10^{12}$	$k = 0$		$k = 1$		$k = 5$	
		Present	Ahmadi [55]	Present	Ahmadi [55]	Present	Ahmadi [55]
20	0	9.7898	9.8296	6.8297	6.9676	5.8508	5.9172
	1	9.3397	9.3776	6.5158	6.6473	5.5818	5.6452
	2	8.9465	8.9829	6.2415	6.3675	5.3469	5.4075
	3	8.5991	8.6341	5.9991	6.1203	5.1392	5.1975
	4	8.2893	8.3230	5.7830	5.8998	4.9541	5.0103
	5	8.0107	8.0433	5.5886	5.7016	4.7876	4.8419
50	0	9.8235	9.8633	6.8540	6.9919	5.8737	5.9390
	1	9.3719	9.4098	6.5389	6.6704	5.6036	5.6660
	2	8.9773	9.0137	6.2636	6.3896	5.3677	5.4274
	3	8.6287	8.6637	6.0204	6.1415	5.1593	5.2167
	4	8.3178	8.3516	5.8035	5.9203	4.9734	5.0288
	5	8.0383	8.0709	5.6085	5.7213	4.8063	4.8598
100	0	9.8283	9.8683	6.8575	6.9955	5.8770	5.9421
	1	9.3765	9.4147	6.5422	6.6739	5.6068	5.6689
	2	8.9817	9.0183	6.2668	6.3929	5.3707	5.4303
	3	8.6330	8.6682	6.0235	6.1447	5.1622	5.2195
	4	8.3220	8.3558	5.8065	5.9233	4.9762	5.0314
	5	8.0423	8.0750	5.6113	5.7242	4.8090	4.8623

Table 3 The first six non-dimensional frequencies of the FG porous nanobeams against different nonlocal parameters and porosity distributions

Porosity	k	Frequency	$\mu = 0$	$\mu = 0.5$	$\mu = 1$	$\mu = 2$	$\mu = 3$	$\mu = 4$
Type I	1	Ω_1	9.0364	8.8213	8.6209	8.2580	7.9374	7.6514
		Ω_2	34.6899	31.7019	29.3731	25.9316	23.4716	21.6006
		Ω_3	73.5181	61.1774	53.5011	44.1208	38.4034	34.4542
		Ω_4	121.7681	91.0247	75.8222	59.7141	50.8365	45.0174
		Ω_5	176.3795	118.0145	94.7209	72.4011	60.8487	53.4984
		Ω_6	235.1791	141.1392	110.2166	82.6023	68.8755	60.2979
	5	Ω_1	10.0244	9.7859	9.5636	9.1609	8.8052	8.4880
		Ω_2	37.7436	34.4925	31.9587	28.2143	25.5377	23.5020
		Ω_3	78.1233	65.0095	56.8524	46.8845	40.8090	36.6125
		Ω_4	126.4561	94.5292	78.7413	62.0131	52.7937	46.7506
		Ω_5	179.4886	120.0949	96.3906	73.6773	61.9213	54.4415
		Ω_6	235.2477	141.1803	110.2488	82.6264	68.8956	60.3155
Type II	1	Ω_1	8.1195	7.9263	7.7463	7.4201	7.1320	6.8751
		Ω_2	31.3491	28.6488	26.5443	23.4342	21.2111	19.5203
		Ω_3	66.9333	55.6979	48.7092	40.1690	34.9637	31.3683
		Ω_4	111.7101	83.5062	69.5593	54.7818	46.6374	41.2990
		Ω_5	162.9507	109.0294	87.5093	66.8887	56.2160	49.4253
		Ω_6	218.6144	131.1981	102.4536	76.7843	64.0243	56.0509
	5	Ω_1	8.0583	7.8665	7.6878	7.3641	7.0782	6.8232
		Ω_2	30.8409	28.1844	26.1140	23.0544	20.8673	19.2039
		Ω_3	65.1994	54.2550	47.4474	39.1284	34.0580	30.5557
		Ω_4	107.7875	80.5739	67.1168	52.8582	44.9998	39.8488
		Ω_5	155.9177	104.3237	83.7324	64.0018	53.7897	47.2921
		Ω_6	207.7054	124.6512	97.3411	72.9527	60.8294	53.2539
Type III	1	Ω_1	9.0981	8.8816	8.6798	8.3144	7.9916	7.7036
		Ω_2	34.7471	31.7541	29.4215	25.9743	23.5102	21.6362
		Ω_3	73.1674	60.8855	53.2459	43.9103	38.2202	34.2899
		Ω_4	120.4080	90.0080	74.9753	59.0472	50.2687	44.5146
		Ω_5	173.3913	116.0152	93.1162	71.1745	59.8178	52.5921
		Ω_6	230.0282	138.0479	107.8026	80.7932	67.3670	58.9773
	5	Ω_1	9.2547	9.0344	8.8292	8.4575	8.1291	7.8362
		Ω_2	34.8009	31.8033	29.4670	26.0145	23.5466	21.6697
		Ω_3	72.0063	59.9194	52.4010	43.2135	37.6137	33.7457
		Ω_4	116.5705	87.1394	72.5857	57.1652	48.6666	43.0958
		Ω_5	165.5186	110.7476	88.8884	67.9429	57.1019	50.2042
		Ω_6	217.0432	130.2552	101.7173	76.2324	63.5642	55.6480
Type IV	1	Ω_1	8.0352	7.8440	7.6658	7.3431	7.0580	6.8037
		Ω_2	31.1406	28.4583	26.3677	23.2784	21.0700	19.3905
		Ω_3	66.8160	55.6003	48.6238	40.0986	34.9024	31.3133
		Ω_4	112.0939	83.7930	69.7983	54.9699	46.7976	41.4409
		Ω_5	164.3132	109.9411	88.2410	67.4480	56.6860	49.8386
		Ω_6	221.4069	132.8740	103.7623	77.7651	64.8421	56.7668
	5	Ω_1	8.7427	8.5346	8.3408	7.9896	7.6794	7.4027
		Ω_2	33.4850	30.6008	28.3529	25.0309	22.6563	20.8503
		Ω_3	70.7589	58.8813	51.4932	42.4649	36.9621	33.1611
		Ω_4	116.8492	87.3478	72.7593	57.3019	48.7829	43.1989
		Ω_5	168.7860	112.9338	90.6430	69.2840	58.2291	51.1952
		Ω_6	224.5057	134.7337	105.2145	78.8535	65.7497	57.5613

For uneven porosity distribution [42]:

$$\begin{aligned} E(z) &= \left[E_{\mathrm{m}} + (E_{\mathrm{c}} - E_{\mathrm{m}})\left(\frac{1}{2} + \frac{z}{h}\right)^k\right] - \frac{1}{2}P_0(E_{\mathrm{c}} + E_{\mathrm{m}})\left(1 - \frac{2|z|}{h}\right) \\ \rho(z) &= \left[\rho_{\mathrm{m}} + (\rho_{\mathrm{c}} - \rho_{\mathrm{m}})\left(\frac{1}{2} + \frac{z}{h}\right)^k\right] - \frac{1}{2}P_0(\rho_{\mathrm{c}} + \rho_{\mathrm{m}})\left(1 - \frac{2|z|}{h}\right) \end{aligned} \tag{32}$$

The material gradient index is taken to be $k = 2$, and the non-dimensional frequency of the beam is expressed as follows:

Table 4 The high frequencies of the FG porous nanobeams against different nonlocal parameters and porosity distributions

Porosity	k	Frequency	$\mu = 0$	$\mu = 0.5$	$\mu = 1$	$\mu = 2$	$\mu = 3$	$\mu = 4$
Type I	1	Ω_{10}	490.0181	201.1449	148.6296	107.6009	88.5705	77.0194
		Ω_{50}	3548.9549	318.2311	225.4770	159.5975	130.3547	112.9096
		Ω_{100}	8678.9583	390.2951	276.1200	195.2957	159.4718	138.1124
		Ω_{200}	20071.3064	451.6487	319.4043	225.8673	184.4237	159.7173
	5	Ω_{10}	469.3590	192.6646	142.3634	103.0645	84.8363	73.7723
		Ω_{50}	3457.4547	310.0263	219.6637	155.4827	126.9939	109.9985
		Ω_{100}	8609.0636	387.1520	273.8963	193.7229	158.1875	137.0002
		Ω_{200}	19256.5369	433.3146	306.4385	216.6985	176.9373	153.2338
Type II	1	Ω_{10}	463.3523	190.1990	140.5415	101.7455	83.7506	72.8282
		Ω_{50}	3527.9217	316.3450	224.1407	158.6516	129.5822	112.2404
		Ω_{100}	8746.2411	393.3209	278.2606	196.8097	160.7080	139.1831
		Ω_{200}	20191.1080	454.3445	321.3108	227.2154	185.5245	160.6706
	5	Ω_{10}	432.5629	177.5604	131.2026	94.9846	78.1855	67.9888
		Ω_{50}	3245.4518	291.0163	206.1945	145.9489	119.2069	103.2536
		Ω_{100}	7597.7810	341.6743	241.7225	170.9669	139.6056	120.9071
		Ω_{200}	16210.1591	364.7644	257.9600	182.4168	148.9459	128.9923
Type III	1	Ω_{10}	473.1053	194.2024	143.4997	103.8871	85.5135	74.3611
		Ω_{50}	3512.8359	314.9923	223.1823	157.9732	129.0281	111.7604
		Ω_{100}	8723.4312	392.2951	277.5349	196.2965	160.2889	138.8201
		Ω_{200}	19819.2162	445.9761	315.3927	223.0304	182.1074	157.7113
	5	Ω_{10}	434.0362	178.1652	131.6495	95.3081	78.4518	68.2204
		Ω_{50}	3189.8489	286.0304	202.6618	143.4484	117.1646	101.4846
		Ω_{100}	7584.4704	341.0757	241.2990	170.6673	139.3611	120.6953
		Ω_{200}	16284.9307	366.4469	259.1499	183.2583	149.6329	129.5873
Type IV	1	Ω_{10}	474.7890	194.8936	144.0104	104.2568	85.8178	74.6258
		Ω_{50}	3499.4651	313.7934	222.3328	157.3719	128.5370	111.3350
		Ω_{100}	8448.7403	379.9422	268.7956	190.1153	155.2416	134.4489
		Ω_{200}	19474.6087	438.2217	309.9088	219.1525	178.9410	154.9691
	5	Ω_{10}	464.9077	190.8375	141.0132	102.0871	84.0318	73.0727
		Ω_{50}	3496.5205	313.5293	222.1457	157.2395	128.4288	111.2414
		Ω_{100}	8726.4373	392.4303	277.6305	196.3641	160.3442	138.8680
		Ω_{200}	19988.1164	449.7768	318.0805	224.9311	183.6593	159.0553

Table 5 The variation of non-dimensional frequencies of FG porous nanobeams against ratio *L/h*

Porosity	Frequency	L/h					
		10	20	30	40	50	100
Type I	Ω_1	8.2580	4.1750	2.7891	2.0934	1.6753	0.8380
	Ω_{10}	107.6009	77.4699	58.4555	46.2953	38.0913	19.8439
	Ω_{100}	195.2957	159.7255	145.0365	137.0456	131.3606	110.2896
	Ω_{200}	225.8673	195.3350	173.3906	159.7592	151.0484	131.3881
Type II	Ω_1	7.4201	3.7453	2.5013	1.8771	1.5021	0.7514
	Ω_{10}	101.7455	71.5717	53.3568	41.9881	34.4227	17.8305
	Ω_{100}	196.8097	158.7770	142.1942	133.1131	126.7501	104.2879
	Ω_{200}	227.2154	196.8487	173.7610	158.8096	149.0211	126.7764
Type III	Ω_1	8.3144	4.2107	2.8139	2.1122	1.6905	0.8457
	Ω_{10}	103.8871	76.2079	58.0936	46.2593	38.1792	19.9876
	Ω_{100}	196.2965	158.0954	141.1708	132.2385	126.2988	106.6020
	Ω_{200}	223.0304	196.2938	173.3820	158.1260	148.0992	126.3339
Type IV	Ω_1	7.3431	3.7019	2.4717	1.8548	1.4842	0.7424
	Ω_{10}	104.2568	72.1314	53.3248	41.7859	34.1776	17.6403
	Ω_{100}	190.1153	157.4393	144.0187	136.2331	130.2796	106.7449
	Ω_{200}	219.1525	190.0952	169.7720	157.4429	149.5587	130.2930

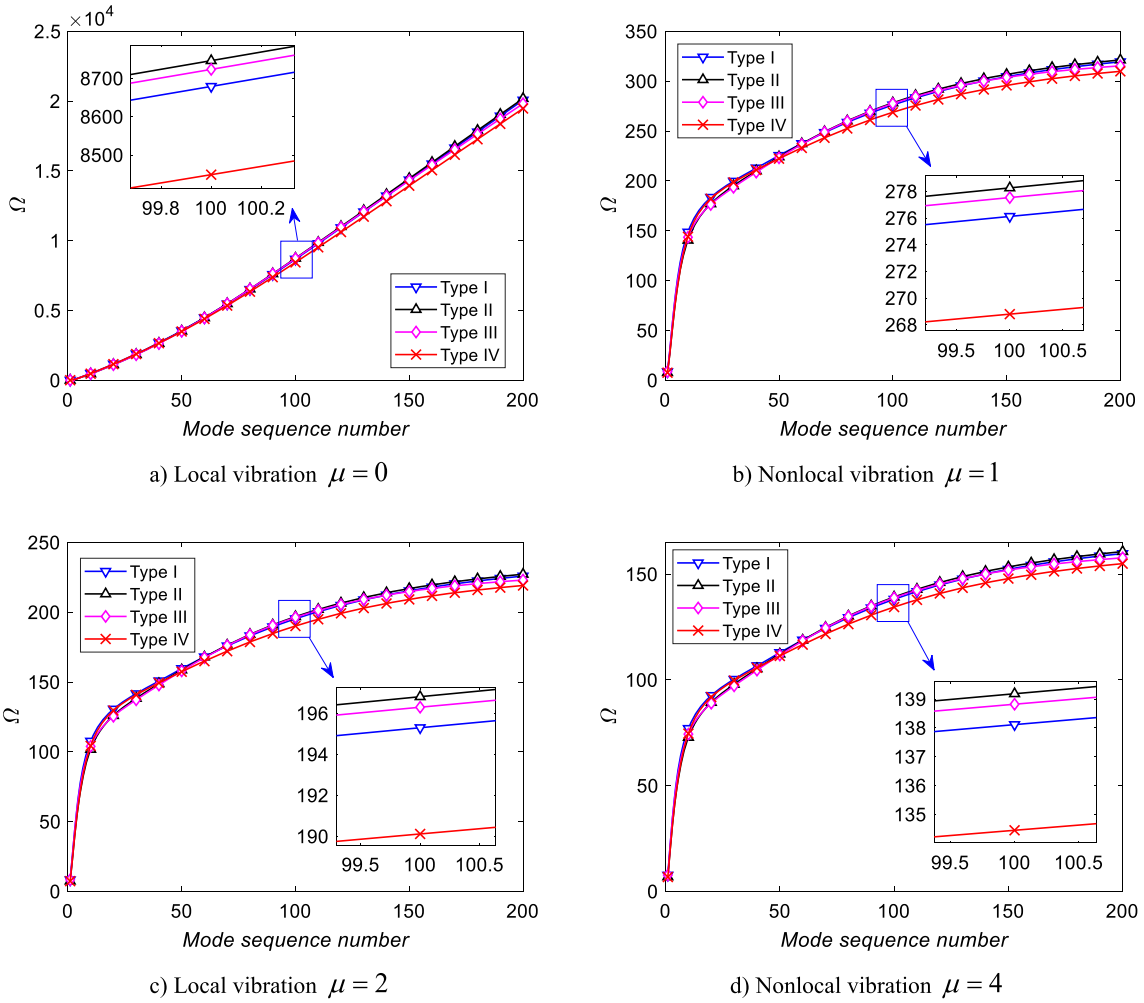

Fig. 4 The variation of the non-dimensional frequency of the FG porous nanobeams for $L/h = 10$, $k = 1$, $P_0 = 0.5$ against different values of nonlocal parameters

$$\overline{\omega} = \omega \frac{L^2}{h} \sqrt{\frac{\rho_{\mathrm{m}}}{E_{\mathrm{m}}}} \tag{33}$$

Table 1 compares the numerical results from the current study with those of Hadji et al. [42] using two types of porosity distributions and L/h ratios. It is noticed that the results of Hadji et al. [42] are found using NET and hyperbolic shear deformation theory, in which the hyperbolic function was used to describe the nonlinear variation of the transverse shear strain through the thickness of the nanobeam. The results of the current study and those of Hadji et al. [42] are in good agreement, as shown in Table 1.

Secondly, the free vibration of the simply supported FG nanobeams is considered. The beam is made from Al_2O_3 as ceramic phase and Fe as metal phase. The material properties of the ceramic and metal phases are: $E_{\mathrm{c}} = 390$ GPa, $\rho_{\mathrm{c}} = 3960$ kg/m^3, $\nu_{\mathrm{c}} = 0.24$; $E_{\mathrm{m}} = 210$ GPa, $\rho_{\mathrm{m}} = 7800$ kg/m^3, $\nu_{\mathrm{m}} = 0.3$. The beam's length is $L = 10,000$ nm. The non-dimensional frequency of the FG nanobeams is found as:

$$\omega* = \omega L^2 \sqrt{\frac{\rho_{\mathrm{c}} A}{E_{\mathrm{c}} I}}, \; A = bh, \; I = \frac{bh^3}{12} \tag{34}$$

Table 2 compares the present results regarding the non-dimensional fundamental natural frequency of the FG nanobeams versus different L/h ratios and nonlocal parameter with the results of Ahmadi [55]. From

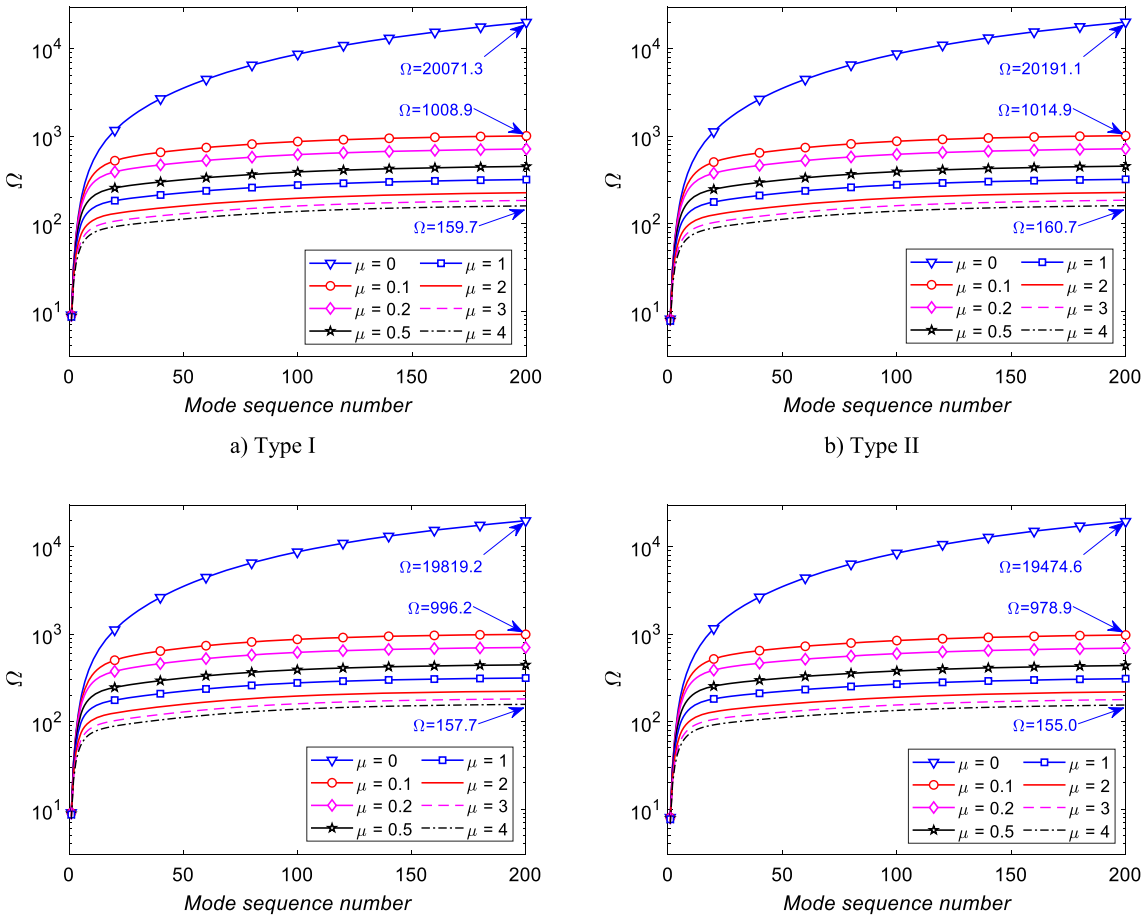

a) Type I b) Type II

c) Type III d) Type IV

Fig. 5 The variation of the non-dimensional frequency of the FG porous nanobeams with $L/h = 10$, $k = 1$, $P_0 = 0.5$ versus different types of porosity distributions

Table 2, it is observed that the present results are coincide with the results of Ahmadi [55]. It is noticed that there is a slight difference between the present results and Ahmadi's results. Because the present results are obtained via higher-order shear deformation theory and analytical solution, while the results of Ahmadi are found using first-order shear deformation theory and meshless method.

4.2 Parameter study

A simply supported FG porous nanobeams with the length of $L = 10$ nm, the depth of $b = 1$ nm, and the height of h is considered in this parametric study. The FG porous nanobeams are made from ceramic phase and metal phase with the material properties of $E_c = 14.4 \times 10^9$ Pa, $\rho_c = 12.2 \times 10^3$ kg/m^3, $\nu_c = 0.38$, $E_m = 1.44 \times 10^9$ Pa, $\rho_m = 1.22 \times 10^3$ kg/m^3, $\nu_m = 0.38$. The subsequent non-dimensional quantities are considered for convenience:

$$\Omega = \omega L^2 \sqrt{\frac{\rho_c A}{E_c I}};\ A = bh_0\ ; I = \frac{bh_0^3}{12};\ h_0 = \frac{L}{10} \tag{35}$$

Table 3 examines the effects of the nonlocal parameter on the low-frequency vibration of FG porous nanobeams for $L/h = 10$, $P_0 = 0.5$. It is observed that when the nonlocal parameter is considered, the frequencies of the FG porous nanobeams are lower than the local beams ($\mu = 0$). As the nonlocal parameter increases, the non-dimensional frequency of the FG porous nanobeams decrease for all cases of porosity distributions and power-law indexes.

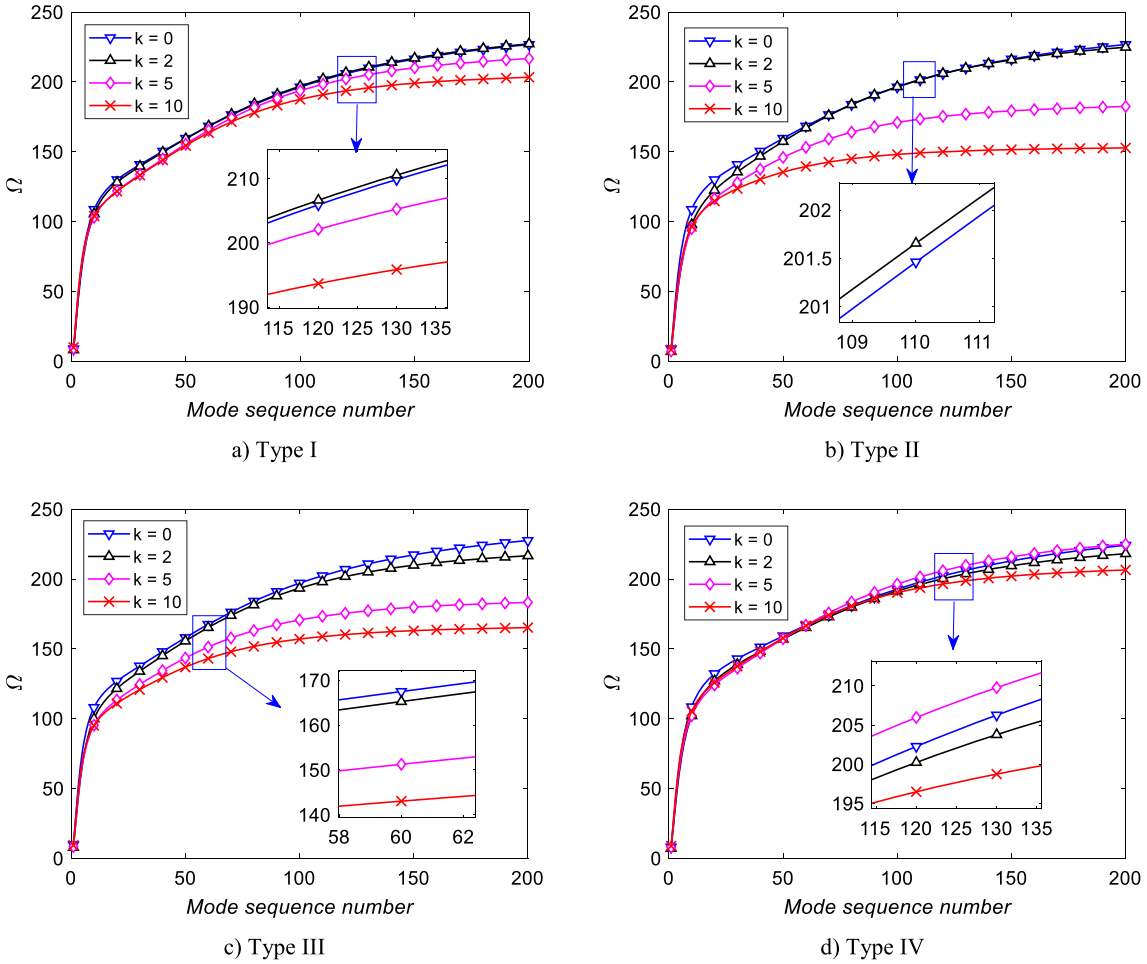

Fig. 6 The variation of the non-dimensional frequency of the FG porous nanobeams with $L/h = 10$, $P_0 = 0.5$, $\mu = 2$ versus different values of power-law index

Next, the four frequencies for 10th, 50th, 100th, and 200th modes of the FG porous nanobeams are presented in Table 4 with $L/h = 10$, $P_0 = 0.5$. By comparing these two tables, the frequencies of the FG porous nanobeams increase rapidly when the mode number increases. Again, when the nonlocal parameter increases, the frequencies of the FG porous nanobeams decrease rapidly. It is noticed that the effects of the nonlocal parameter on the high-frequency vibration of the FG porous nanobeams are more significant than on the low frequency. For example, the non-dimensional frequency of the FG porous nanobeams of type I with $\mu = 0$, $k = 1$ is 18% greater than the those with $\mu = 4$, while the frequency of 100th mode of the FG porous nanobeams with $\mu = 0$, $k = 1$ is 6100% greater than those with $\mu = 4$, and the difference being 12,400% for the 200th mode.

Table 5 examines the effect of the ratio L/h on the non-dimensional frequencies of the FG porous nanobeams for $k = 1$, $P_0 = 0.5$, $\mu = 2$. According to this table, as the ratio L/h rises, the non-dimensional frequencies of the FG porous nanobeams are reduced for all cases of porosity distribution, both low- and high-frequency vibration. The non-dimensional fundamental frequencies of the FG porous nanobeams with $L/h = 10$ are 9–10 times greater than those for FG porous nanobeams with $L/h = 100$. For 10th mode, the non-dimensional fundamental frequencies of the FG porous nanobeams with $L/h = 10$ is 4–6 times greater than that of such FG porous nanobeams with $L/h = 100$. For 100th and 200th modes, the frequency of the FG porous nanobeams with $L/h = 10$ is $1 - 2$ times greater than that of such FG porous nanobeams with $L/h = 100$.

Figure 4 illustrates the variation of the non-dimensional frequencies of the FG porous nanobeams concerning to the mode numbers for different porosity distributions and nonlocal parameters. It is observed that the non-dimensional frequencies of the FG porous nanobeams increases rapidly with the increase of mode

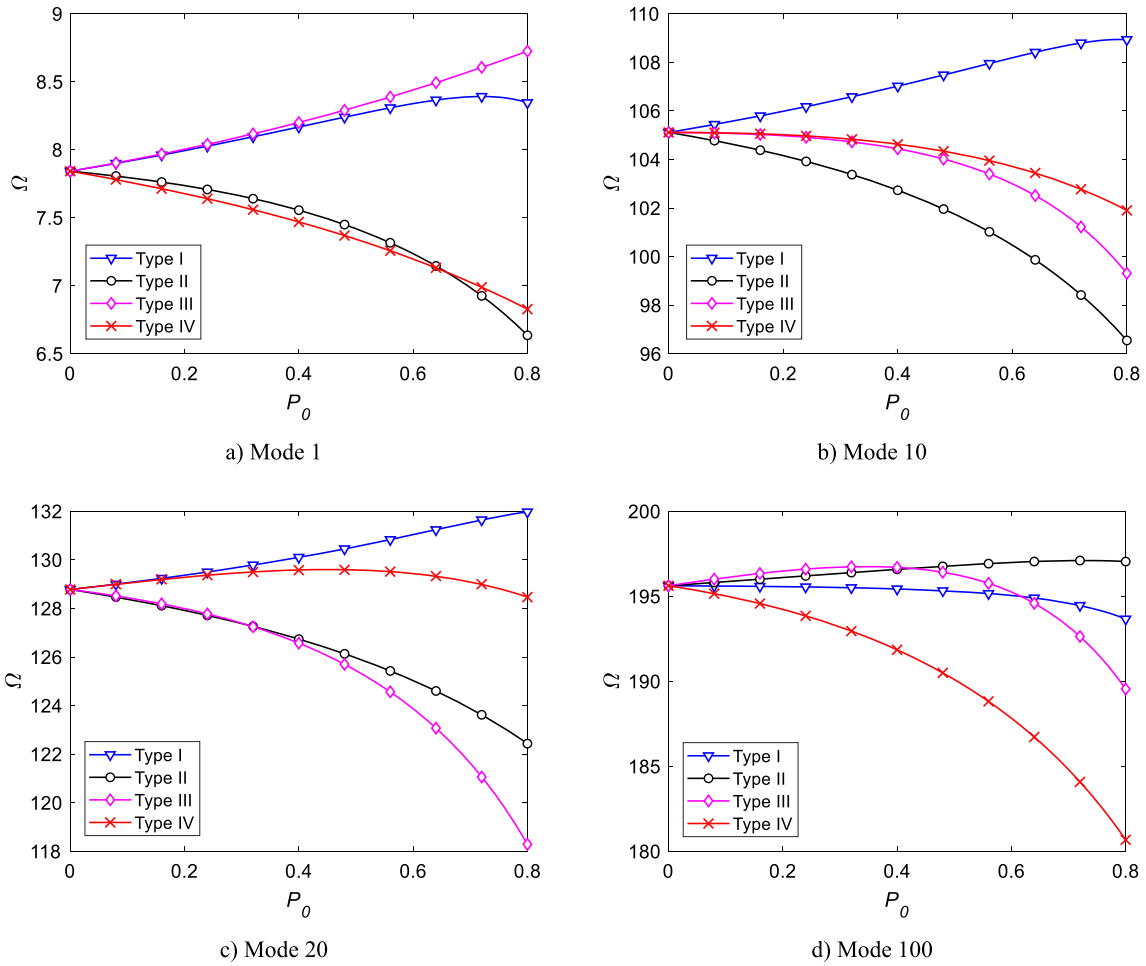

a) Mode 1 b) Mode 10

c) Mode 20 d) Mode 100

Fig. 7 The variation of the non-dimensional frequency of the FG porous nanobeams versus P_0 for $L/h = 10, k = 1, \mu = 2$

number, and the difference in the non-dimensional frequencies of the four types of porosity distribution is low. The non-dimensional frequencies of the FG porous nanobeams with type II porosity are the highest ones, while the non-dimensional frequencies of the FG porous nanobeams with type IV porosity are the lowest ones. On the other hand, it is concluded that the effects of the nonlocal parameters are significant on the vibration of the FG porous nanobeams. For local vibration ($\mu = 0$), the non-dimensional frequency of the FG porous increase more quickly than those for nonlocal vibration of the FG porous nanobeams ($\mu > 0$).

More details on the effects of the nonlocal parameter on the high-frequency vibration of the FG porous nanobeams are illustrated in Fig. 5. Again, it is found that the influence of the type of the porosity distribution is low, while the effects of the nonlocal parameters on the vibration of the FG porous nanobeams are noteworthy, especially for high frequencies of the FG porous nanobeams. For example, the local frequencies ($\mu = 0$) of 200th modes are approximately 2000% greater than those of nonlocal frequencies with $\mu = 0.1$, and are approximately 16,000% greater than those of nonlocal frequencies with $\mu = 4$.

Continuously, the variation of the non-dimensional frequencies of the FG porous nanobeams with different values of the power-law index is demonstrated in Fig. 6. As shown in Fig. 6, the influence of the power-law index on the free vibration behaviors of FG porous nanobeams is dependent on the kind of porosity distribution. Because both porosity distribution and power-law index effect on the mass density and rigidity of the FG porous nanobeams. Therefore, it should be noticed this couple-effects between the power-law index and the type of the porosity distribution in design, testing and manufacture the FG porous nanodevices.

The influence of the porosity coefficient P_0 on the non-dimensional frequencies of the FG porous nanobeams with four types of porosity distribution are investigated in Fig. 7 for 1st, 10th, 20th, and 100th modes. It is obvious that the variation of the non-dimensional frequencies of the FG porous nanobeams not only depends

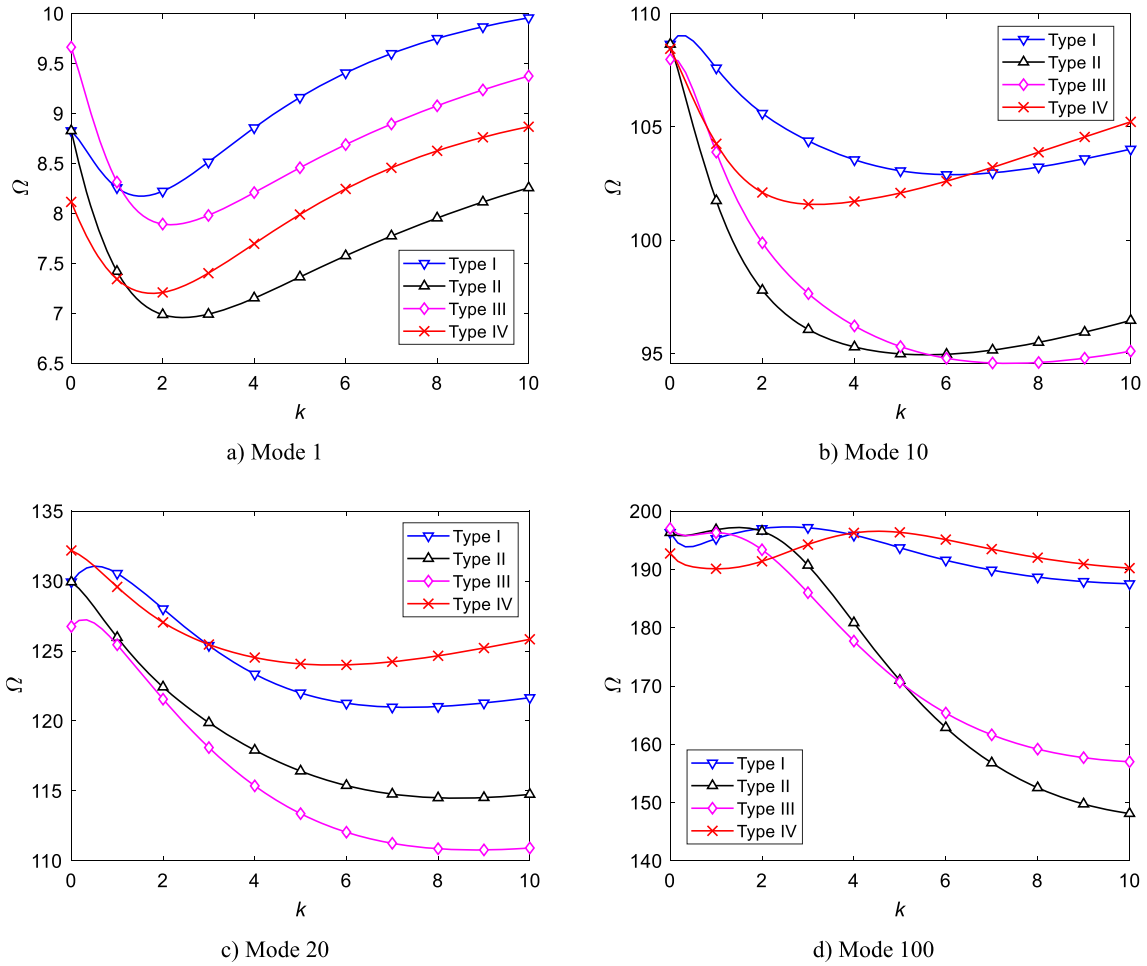

Fig. 8 The variation of the non-dimensional frequency of the FG porous nanobeams versus k for $L/h = 10$, $P_0 = 0.5$, $\mu = 2$

on the variation of the porosity coefficient but also the mode of the vibration of the FG porous nanobeams. For the 1st mode, when the porosity coefficient increases, the non-dimensional frequencies of the FG porous nanobeams increase for type I and type III of the porosity distribution, while the non-dimensional frequencies of the FG porous nanobeams decrease for type II and type IV of the porosity distribution. For the 10th mode, when the porosity coefficient increases, the non-dimensional frequencies of the FG porous nanobeams of type I increase, while the frequencies of the FG porous nanobeams of types II, III, and IV decrease. In the case of the 20th mode, when the porosity coefficient increases, the non-dimensional frequencies of the FG porous nanobeams of type I increase, the non-dimensional frequencies of type II and III decrease, while the non-dimensional frequencies of type IV increase when the P_0 increases from 0 to 0.6, then the non-dimensional frequencies decrease as the increase of P_0 from 0.6 to 0.8. In the cases of the 100th mode, when the coefficient P_0 increase, the non-dimensional frequencies of types I and II increase, and the non-dimensional frequencies of type IV decrease, but the non-dimensional frequencies of type III increase when P_0 increase from 0 to 0.4, then the frequencies decrease as increase of P_0 from 0.4 to 0.8.

Figure 8 examines the influence of the power-law index k on the vibration behaviors of the FG porous nanobeams. According to Fig. 8, it is found that the influences of the power-law index are complex, and it depends on the mode numbers. When the k increases from 0 to 2, the non-dimensional fundamental frequencies of the FG porous nanobeams decrease rapidly, then the non-dimensional fundamental frequencies increase with the increase of the k from 2 to 10. Besides, the effects of the power-law index on the fundamental frequencies of the FG porous nanobeams with four types of porosity distribution are approximated. For high-frequency vibration, when the k increases, the non-dimensional frequencies of the FG porous nanobeams also decrease and then increase; however, some maximum and minimum values appear. Additionally, the effects

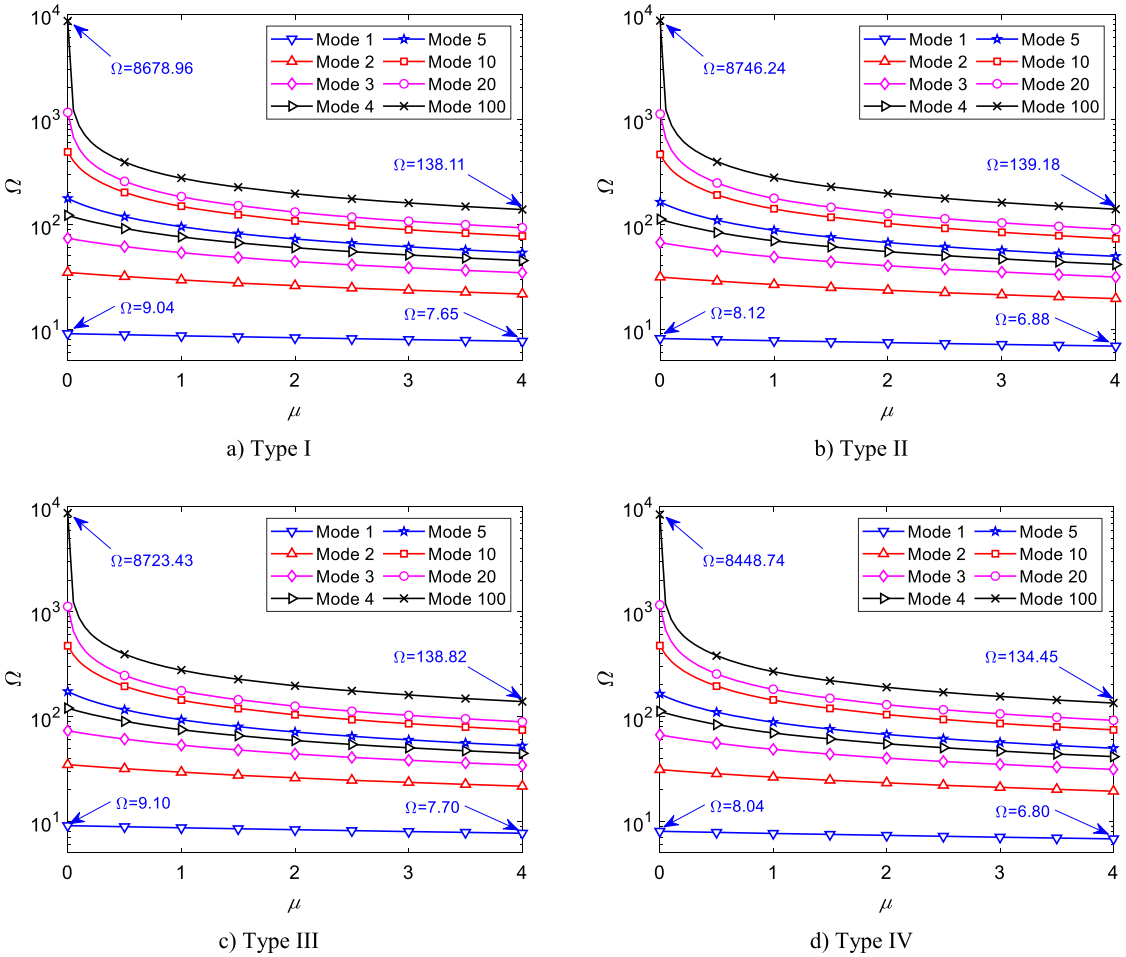

a) Type I b) Type II

c) Type III d) Type IV

Fig. 9 The variation of the non-dimensional frequency of the FG porous nanobeams against μ for $L/h = 10$, $P_0 = 0.5$, $k = 1$

of the power-law index on the high frequencies of the FG porous nanobeams depend significantly on the porosity distributions. The reason is that when the power-law index increases, both effective mass density and Young's modulus decrease; therefore, the variation of the fundamental frequencies of the FG porous nanobeams is more complex. Consequently, the vibration behaviors of the FG porous nanobeams undergoing high-frequency conditions should be analyzed carefully. When $k = 0$, the FG porous nanobeams become the homogeneous isotropic ones, and the non-dimensional frequencies of such beams of type I and II are identical.

Lastly, the influence of the nonlocal parameter on the behaviors of the FG porous nanobeams is studied for some vibration modes and different types of porosity distribution in Fig. 9. For both low- and high-frequency vibration of the FG porous nanobeams, the nonlocal parameter reduces the non-dimensional frequencies of such beams. For low-frequency vibration, the non-dimensional frequencies of the FG porous nanobeams decrease linearly as the increase of the nonlocal parameter. For high-frequency vibration, the non-dimensional frequencies of the FG porous nanobeams decrease nonlinearly as the increase of the nonlocal parameter. When the nonlocal parameter increases from 0 to 0.5, the non-dimensional frequencies of the FG porous nanobeams decrease rapidly, and the speed of the decrease slowdown when the nonlocal parameter increase from 0.5 to 4.

5 Conclusions

This work presented a thorough examination of the free vibration behavior of FG porous nanobeams in low- and high-frequency conditions. Higher-order shear deformation theory and nonlocal elasticity theory were used to develop the governing equations. To solve the system of equations of motion, the Navier closed-form solution was utilized, and the numerical results were compared to published data to check the correctness of

the suggested approach. The computed program was then employed to generate the FG porous nanobeams' low- and high-frequency vibration. Some major conclusions may be drawn from the numerical results, which are as follows:

- When the nonlocal parameter is included, the non-dimensional frequencies of the FG porous nanobeams are reduced, especially for high modes.
- The effects of the porosity depend on the type of the distribution and the power-law index, it can improve or reduce the non-dimensional frequencies of the FG porous nanobeams and should be considered carefully in practice.
- The effects of the power-law index on the high-frequency of the FG porous nanobeams are also more complex than on the low-frequency vibration of such beams.

The current finding can serve as a benchmark result for the design, testing, optimization, and use of the FG porous nanobeams as well as high-frequency behaviors of the structures with different geometries.

Author contribution MHG analyzed methodology, visualization, software, writing—reviewing and editing, and funding acquisition. AA provided data curation, visualization, and writing—reviewing and editing. MA developed software, validation, and writing—reviewing and editing. PVV performed conceptualization, investigation, software, visualization, formal analysis, validation, writing—original draft preparation, writing—reviewing and editing, and project administration. All authors reviewed the manuscript.

Funding This project was funded by Deanship of Scientific research (DSR) from Jazan University, Jazan, Kingdom of Saudi Arabia, under grant number W43-075. The authors acknowledge DSR with thanks for technical and financial support.

Declarations

Conflict of interest The authors declare that they have no known competing financial interests or personal relationships that could have appeared to influence the work reported in this paper.

References

1. Thai, H.T., Kim, S.E.: A review of theories for the modeling and analysis of functionally graded plates and shells. Compos. Struct. **128**, 70 (2015). https://doi.org/10.1016/j.compstruct.2015.03.010
2. Saleh, B., Jiang, J., Fathi, R., Al-hababi, T., Xu, Q., Wang, L., Song, D., Ma, A.: 30 Years of functionally graded materials: an overview of manufacturing methods, applications and future challenges. Compos. Part B Eng. **201**, 108376 (2020). https://doi.org/10.1016/j.compositesb.2020.108376
3. Bagheri, R., Tadi Beni, Y.: On the size-dependent nonlinear dynamics of viscoelastic/flexoelectric nanobeams. JVC/J. Vib. Control. **27**, 2018–2033 (2021). https://doi.org/10.1177/1077546320952225
4. Hosseini-Hashemi, S., Fadaee, M., Atashipour, S.R.: Study on the free vibration of thick functionally graded rectangular plates according to a new exact closed-form procedure. Compos. Struct. **93**, 722–735 (2011). https://doi.org/10.1016/j.compstruct.2010.08.007
5. Hosseini-Hashemi, S., Rokni Damavandi Taher, H., Akhavan, H., Omidi, M.: Free vibration of functionally graded rectangular plates using first-order shear deformation plate theory. Appl. Math. Model. **34**, 1276–1291 (2010). https://doi.org/10.1016/j.apm.2009.08.008
6. Neves, A.M.A., Ferreira, A.J.M., Carrera, E., Cinefra, M., Jorge, R.M.N., Soares, C.M.M.: Static analysis of functionally graded sandwich plates according to a hyperbolic theory considering Zig-Zag and warping effects. Adv. Eng. Softw. **52**, 30–43 (2012). https://doi.org/10.1016/j.advengsoft.2012.05.005
7. Van Vinh, P., Belarbi, M.O., Avcar, M., Civalek, Ö.: An improved first-order mixed plate element for static bending and free vibration analysis of functionally graded sandwich plates. Arch. Appl. Mech. **93**, 1841–1862 (2023). https://doi.org/10.1007/s00419-022-02359-z
8. Van Vinh, P., Huy, L.Q.: Finite element analysis of functionally graded sandwich plates with porosity via a new hyperbolic shear deformation theory. Def. Technol. **18**, 490–508 (2022). https://doi.org/10.1016/j.dt.2021.03.006
9. Van Vinh, P., Avcar, M., Belarbi, M.O., Tounsi, A., Quang Huy, L.: A new higher-order mixed four-node quadrilateral finite element for static bending analysis of functionally graded plates. Structures **47**, 1595–1612 (2023). https://doi.org/10.1016/j.istruc.2022.11.113
10. Eltaher, M.A., Mohamed, N.: Nonlinear stability and vibration of imperfect CNTs by doublet mechanics. Appl. Math. Comput. **382**, 125311 (2020). https://doi.org/10.1016/j.amc.2020.125311
11. Marinca, B., Herisanu, N., Marinca, V.: Investigating nonlinear forced vibration of functionally graded nanobeam based on the nonlocal strain gradient theory considering mechanical impact, electromagnetic actuator, thickness effect and nonlinear foundation. Eur. J. Mech. - A/Solids. **102**, 105119 (2023). https://doi.org/10.1016/j.euromechsol.2023.105119
12. Tadi Beni, Y.: Size dependent coupled electromechanical torsional analysis of porous FG flexoelectric micro/nanotubes. Mech. Syst. Signal Process. **178**, 109281 (2022). https://doi.org/10.1016/j.ymssp.2022.109281

13. Van Vinh, P., Belarbi, M.O., Tounsi, A.: Wave propagation analysis of functionally graded nanoplates using nonlocal higher-order shear deformation theory with spatial variation of the nonlocal parameters. Waves Random Complex Media (2022). https://doi.org/10.1080/17455030.2022.2036387
14. Hoa, L.K., Van Vinh, P., Duc, N.D., Trung, N.T., Son, L.T., Van Thom, D.: Bending and free vibration analyses of functionally graded material nanoplates via a novel nonlocal single variable shear deformation plate theory. Proc. Inst. Mech Eng. Part C J. Mech. Eng. Sci. **235**, 3641–3653 (2021). https://doi.org/10.1177/0954406220964522
15. Sobhy, M.: A comprehensive study on FGM nanoplates embedded in an elastic medium. Compos. Struct. **134**, 966–980 (2015). https://doi.org/10.1016/j.compstruct.2015.08.102
16. Shahverdi, H., Barati, M.R.: Vibration analysis of porous functionally graded nanoplates. Int. J. Eng. Sci. **120**, 82–99 (2017). https://doi.org/10.1016/j.ijengsci.2017.06.008
17. Arefi, M., Zenkour, A.M.: Size-dependent free vibration and dynamic analyses of piezo-electro-magnetic sandwich nanoplates resting on viscoelastic foundation. Phys. B Condens. Matter. **521**, 188–197 (2017). https://doi.org/10.1016/j.physb.2017.06.066
18. Daneshmehr, A., Rajabpoor, A., Hadi, A.: Size dependent free vibration analysis of nanoplates made of functionally graded materials based on nonlocal elasticity theory with high order theories. Int. J. Eng. Sci. **95**, 23–35 (2015). https://doi.org/10.1016/j.ijengsci.2015.05.011
19. Eringen, A.C.: Theory of micropolar plates. Zeitschrift Für Angew. Math. Und Phys. ZAMP. **18**, 12–30 (1967). https://doi.org/10.1007/BF01593891
20. Eringen, A.C.: On differential equations of nonlocal elasticity and solutions of screw dislocation and surface waves. J. Appl. Phys. **54**, 4703–4710 (1983). https://doi.org/10.1063/1.332803
21. Eringen, A.C.: Nonlocal polar elastic continua. Int. J. Eng. Sci. **10**, 1–16 (1972). https://doi.org/10.1016/0020-7225(72)90070-5
22. Eringen, A.C., Edelen, D.G.B.: On nonlocal elasticity. Int. J. Eng. Sci. **10**, 233–248 (1972). https://doi.org/10.1016/0020-7225(72)90039-0
23. Eltaher, M.A., Emam, S.A., Mahmoud, F.F.: Free vibration analysis of functionally graded size-dependent nanobeams. Appl. Math. Comput. **218**, 7406–7420 (2012). https://doi.org/10.1016/j.amc.2011.12.090
24. Thai, H.T., Vo, T.P.: A nonlocal sinusoidal shear deformation beam theory with application to bending, buckling, and vibration of nanobeams. Int. J. Eng. Sci. **54**, 58–66 (2012). https://doi.org/10.1016/j.ijengsci.2012.01.009
25. Rahmani, O., Pedram, O.: Analysis and modeling the size effect on vibration of functionally graded nanobeams based on nonlocal Timoshenko beam theory. Int. J. Eng. Sci. **77**, 55–70 (2014). https://doi.org/10.1016/j.ijengsci.2013.12.003
26. Arefi, M., Zenkour, A.M.: A simplified shear and normal deformations nonlocal theory for bending of functionally graded piezomagnetic sandwich nanobeams in magneto-thermo-electric environment. J. Sandw. Struct. Mater. **18**, 624–651 (2016). https://doi.org/10.1177/1099636216652581
27. Gholami, M., Azandariani, M.G., Ahmed, A.N., Abdolmaleki, H.: Proposing a dynamic stiffness method for the free vibration of bi-directional functionally-graded Timoshenko nanobeams. Adv. Nano Res. **14**, 127–139 (2023). https://doi.org/10.12989/anr.2023.14.2.1274
28. Ebrahimi, F., Barati, M.R.: A third-order parabolic shear deformation beam theory for nonlocal vibration analysis of magneto-electro-elastic nanobeams embedded in two-parameter elastic foundation. Adv. Nano Res. **5**, 313–336 (2017). https://doi.org/10.12989/anr.2017.5.4.313
29. Ebrahimi, F., Fardshad, R.E.: Modeling the size effect on vibration characteristics of functionally graded piezoelectric nanobeams based on Reddy's shear deformation beam theory. Adv. Nano Res. **6**, 113–133 (2018). https://doi.org/10.12989/anr.2018.6.2.113
30. Ebrahimi, F., Fardshad, R.E., Mahesh, V.: Frequency response analysis of curved embedded magneto-electro-viscoelastic functionally graded nanobeams. Adv. Nano Res. **7**, 391–403 (2019). https://doi.org/10.12989/anr.2019.7.6.391
31. Ebrahimi, F., Karimiasl, M., Civalek, Ö., Vinyas, M.: Surface effects on scale-dependent vibration behavior of flexoelectric sandwich nanobeams. Adv. Nano Res. **7**, 77–88 (2019). https://doi.org/10.12989/anr.2019.7.2.077
32. Karami, B., Janghorban, M.: A new size-dependent shear deformation theory for free vibration analysis of functionally graded/anisotropic nanobeams. Thin-Walled Struct. **143**, 106227 (2019). https://doi.org/10.1016/j.tws.2019.106227
33. Aria, A.I., Rabczuk, T., Friswell, M.I.: A finite element model for the thermo-elastic analysis of functionally graded porous nanobeams. Eur. J. Mech. A/Solids. **77**, 103767 (2019). https://doi.org/10.1016/j.euromechsol.2019.04.002
34. Ghobadi, A., Tadi Beni, Y., Kamil Żur, K.: Porosity distribution effect on stress, electric field and nonlinear vibration of functionally graded nanostructures with direct and inverse flexoelectric phenomenon. Compos. Struct. **259**, 113220 (2021). https://doi.org/10.1016/j.compstruct.2020.113220
35. Ebrahimi, F., Karimiasl, M., Mahesh, V.: Vibration analysis of magneto-flexo-electrically actuated porous rotary nanobeams considering thermal effects via nonlocal strain gradient elasticity theory. Adv. Nano Res. **7**, 221–229 (2019). https://doi.org/10.12989/anr.2019.7.4.221
36. Wang, S., Kang, W., Yang, W., Zhang, Z., Li, Q., Liu, M., Wang, X.: Hygrothermal effects on buckling behaviors of porous bi-directional functionally graded micro-/nanobeams using two-phase local/nonlocal strain gradient theory. Eur. J. Mech. A/Solids **94**, 104554 (2022). https://doi.org/10.1016/j.euromechsol.2022.104554
37. Wang, S., Ding, W., Li, Z., Xu, B., Zhai, C., Kang, W., Yang, W., Li, Y.: A size-dependent quasi-3D model for bending and buckling of porous functionally graded curved nanobeam. Int. J. Eng. Sci. **193**, 103962 (2023). https://doi.org/10.1016/j.ijengsci.2023.103962
38. Faghidian, S.A., Żur, K.K., Reddy, J.N., Ferreira, A.J.M.: On the wave dispersion in functionally graded porous Timoshenko-Ehrenfest nanobeams based on the higher-order nonlocal gradient elasticity. Compos. Struct. **279**, 114819 (2022). https://doi.org/10.1016/j.compstruct.2021.114819
39. Civalek, Ö., Uzun, B., Yaylı, M.Ö.: On nonlinear stability analysis of saturated embedded porous nanobeams. Int. J. Eng. Sci. **190**, 103898 (2023). https://doi.org/10.1016/j.ijengsci.2023.103898
40. Rastehkenari, S.F., Ghadiri, M.: Nonlinear random vibrations of functionally graded porous nanobeams using equivalent linearization method. Appl. Math. Model. **89**, 1847–1859 (2021). https://doi.org/10.1016/j.apm.2020.08.049

41. Chandel, V.S., Talha, M.: Vibration analysis of functionally graded porous nano-beams: a comparison study. Mater. Today Proc. (2023). https://doi.org/10.1016/j.matpr.2023.03.703
42. Hadji, L., Avcar, M.: Nonlocal free vibration analysis of porous FG nanobeams using hyperbolic shear deformation beam theory. Adv. Nano Res. **10**, 281–293 (2021). https://doi.org/10.12989/anr.2021.10.3.281
43. Akbas, S.D.: Forced vibration analysis of functionally graded nanobeams. Int. J. Appl. Mech. **9**, 1750100 (2017). https://doi.org/10.1142/S1758825117501009
44. Numanoğlu, H.M., Ersoy, H., Akgöz, B., Civalek, Ö.: A new eigenvalue problem solver for thermo-mechanical vibration of Timoshenko nanobeams by an innovative nonlocal finite element method. Math. Methods Appl. Sci. **45**, 2592–2614 (2022). https://doi.org/10.1002/mma.7942
45. Şimşek, M.: Some closed-form solutions for static, buckling, free and forced vibration of functionally graded (FG) nanobeams using nonlocal strain gradient theory. Compos. Struct. **224**, 111041 (2019). https://doi.org/10.1016/j.compstruct.2019.111041
46. Barati, A., Hadi, A., Nejad, M.Z., Noroozi, R.: On vibration of bi-directional functionally graded nanobeams under magnetic field. Mech. Based Des. Struct. Mach. **50**, 468–485 (2022). https://doi.org/10.1080/15397734.2020.1719507
47. Coskun, S., Kim, J., Toutanji, H.: Bending, free vibration, and buckling analysis of functionally graded porous micro-plates using a general third-order plate theory. J. Compos. Sci. **3**, 15 (2019). https://doi.org/10.3390/jcs3010015
48. Wu, L., Jiang, Z., Liu, J.: Thermoelastic stability of functionally graded cylindrical shells. Compos. Struct. **70**, 60–68 (2005). https://doi.org/10.1016/j.compstruct.2004.08.012
49. Han, Q., Wang, Z., Nash, D.H., Liu, P.: Thermal buckling analysis of cylindrical shell with functionally graded material coating. Compos. Struct. **181**, 171–182 (2017). https://doi.org/10.1016/j.compstruct.2017.08.085
50. Shi, P., Dong, C., Shou, H., Li, B.: Bending, vibration and buckling isogeometric analysis of functionally graded porous microplates based on the TSDT incorporating size and surface effects. Thin-Walled Struct. **191**, 111027 (2023). https://doi.org/10.1016/j.tws.2023.111027
51. Nguyen, T.K., Nguyen, B.D.: A new higher-order shear deformation theory for static, buckling and free vibration analysis of functionally graded sandwich beams. J. Sandw. Struct. Mater. **17**, 613–631 (2015). https://doi.org/10.1177/1099636215589237
52. Thai, S., Thai, H.T., Vo, T.P., Patel, V.I.: A simple shear deformation theory for nonlocal beams. Compos. Struct. **183**, 262–270 (2018). https://doi.org/10.1016/j.compstruct.2017.03.022
53. Nguyen, T.K., Sab, K., Bonnet, G.: Shear correction factors for functionally graded plates. Mech. Adv. Mater. Struct. **14**, 567–575 (2007). https://doi.org/10.1080/15376490701672575
54. Menaa, R., Tounsi, A., Mouaici, F., Mechab, I., Zidi, M., Bedia, E.A.A.: Analytical solutions for static shear correction factor of functionally graded rectangular beams. Mech. Adv. Mater. Struct. **19**, 641–652 (2012). https://doi.org/10.1080/15376494.2011.581409
55. Ahmadi, I.: Vibration analysis of 2D-functionally graded nanobeams using the nonlocal theory and meshless method. Eng. Anal. Bound. Elem. **124**, 142–154 (2021). https://doi.org/10.1016/j.enganabound.2020.12.010